submitted to *The Astrophysical Journal Letters*

A parsec-scale flow associated with the IRAS 16547−4247 radio jet

Kate J. Brooks

Departamento de Astronomía, Universidad de Chile, Casilla 36-D, Santiago, Chile

and European Southern Observatory, Casilla 19001 Santiago, Chile

Guido Garay

Departamento de Astronomía, Universidad de Chile, Casilla 36-D, Santiago, Chile

Diego Mardones

Departamento de Astronomía, Universidad de Chile, Casilla 36-D, Santiago, Chile

and

Leonardo Bronfman

Departamento de Astronomía, Universidad de Chile, Casilla 36-D, Santiago, Chile

ABSTRACT

IRAS 16547−4247 is the most luminous (6.2×10^4 $L_\odot$) embedded young stellar object known to harbor a thermal radio jet. We report the discovery using VLT-ISAAC of a chain of H_2 2.12 μm emission knots that trace a collimated flow extending over 1.5 pc. The alignment of the H_2 flow and the central location of the radio jet implies that these phenomena are intimately linked. We have also detected using TIMMI2 an isolated, unresolved 12 μm infrared source towards the radio jet . Our findings affirm that IRAS 16547−4247 is excited by a single O-type star that is driving a collimated jet. We argue that the accretion mechanism which produces jets in low-mass star formation also operates in the higher mass regime.

Subject headings: ISM: individual (IRAS 16547−4247) — ISM: jets and outflows — stars: formation

1. Introduction

Whether massive stars (B and O-type) form via an accretion process similar to that for low-mass stars (Osorio et al. 1999; McKee & Tan 2003) or instead via collisions with lower-mass stars (Bonnell et al. 1998) is currently under debate. Highly collimated radio jets (Rodríguez 1997; Anglada et al. 1998) and Herbig-Haro (HH) flows (Reipurth et al. 2002) are frequently observed towards young low-mass stars. It is now widely accepted that jets are intimately linked to the accretion process and the formation of both bipolar molecular outflows and HH flows (see review by Reipurth & Bally 2001). The role of collimated jets in massive stars ($M > 8$ $M_{\odot}$) is less certain. In this higher mass regime observations of jets are difficult, primarily because of the greater distances involved and because the evolutionary time scales of such jets are expected to be much shorter.

Garay et al. (2003) recently reported the discovery of a triple radio continuum source associated with IRAS 16547−4247, a young stellar object with a bolometric luminosity of 6.2×10^4 $L_{\odot}$, equivalent to that of a single O8 ZAMS star. The three radio components are aligned in a southeast-northwest direction with the outer components (lobes) symmetrically separated from the central source by an angular distance of ∼20 arcsec. The triple system is centred on the position of the IRAS source and is within a 1.2-mm dust continuum emission core whose properties are similar to other massive star-forming cores (e.g. Garay et al. 2002). The spectral indices between 1.4 and 8.6 GHz are 0.49 for the central source and −0.61 and −0.33 for the two outer components. This is consistent with the central source being a thermal jet and the two outer components being non-thermal emission arising from the working surfaces of the jet as it interacts with the surrounding ambient medium. This is the first reported case of a radio jet associated with a young O-type star.

We have performed a series of infrared observations towards IRAS 16547−4247 to confirm the existence of a collimated flow and to investigate the nature of the powering source.

2. Observations

2.1. Near-infrared Data

Near-infrared images were obtained at the European Southern Observatory in Paranal, Chile, using the ISAAC short wave camera (Cuby et al. 2000) mounted on the ANTU telescope of the Very Large Telescope (VLT). The short wave camera is equipped with a 1024×1024 pixel^2 Rockwell HAWAII Hg:Cd:Te array with a pixel scale of $0''.148$ pixel^{-1}, giving a field of view of $2.5' \times 2.5'$. The observations were performed in service mode during

the night of 2002 August 5 under photometric conditions and with a seeing of 0.6 arcsec. Narrow-band images centred on IRAS 16547−4247 were obtained using filters for the emission lines $H_2$1–0 S(1) 2.12 μm and Brγ 2.16 μm, together with the adjacent continuum at 2.09 μm and 2.19 μm. The total on-source integration times were 22 min for the H_2 2.12 μm and 2.09 μm filters and 17 min for the Brγ 2.16 μm and 2.19 μm filters.

Each frame was acquired using a jitter procedure with individual exposures of ≈ 2 min per frame. For each filter, the stack of individual frames were first corrected for instrumental effects such as flat-field and bias effects and then aligned using a cross-correlation method and averaged. The sky contribution was determined from median-averaging the stack of non-aligned frames and subsequently subtracting the result. Astrometric calibration was done by identifying common stars between the final images and an image from the online STScI Digitised Sky Survey. We estimate the positional uncertainty to be less than 1 arcsec.

Photometric calibration of the H_2 2.12 μm data was achieved by observing HIP 080178. The final H_2 2.12 μm image has a 1-σ rms noise level of 1×10^{-16} erg s^{-1} cm^{-2} arcsec^{-2}. The 2.09 μm image was utilised to remove the continuum contribution (stars) from the final H_2 2.12 μm image. A perfect subtraction is impossible because of small misalignments and differences in the PSF between the two filters.

2.2. Mid-infrared Data

Mid-infrared images were obtained at the European Southern Observatory in La Silla, Chile, using the TIMMI2 mid-infrared camera (Reimann et al. 2000) mounted on the 3.6-m telescope. TIMMI2 is equipped with a 320×240 pixel^2 Raytheon Si:As array. A pixel scale of $0.3''$pixel^{-1} was used, giving a field of view of $96'' \times 72''$. The observations were made on the night of 2002 August 10 under photometric conditions and with a seeing of $0.6''$. Images were centred on IRAS 16547−4247 and obtained using the N11.9 μm filter.

A chop-nod procedure was used with a nod duration of ≈ 4 min. The chop and nod amplitudes were 15 arcsec, both oriented north–south. Corrections for sky contribution and instrumental effects were made by computing the double-difference of each chop-nod cycle. An additional bias correction was applied to each of the chopped images. The final image was constructed by shifting and adding all sources in each chop-nod frame. The total on-source integration time was equivalent to 22 min.

Photometric calibration was achieved by observing HD 178345 and HD 4128. The final TIMMI2 image has a 1-σ rms noise level of 0.02 Jy arcsec^{-2}. No astrometric calibration was possible since there were no other sources in the field. We estimate the telescope pointing

accuracy to be less than 5 arcsec.

3. Results & Discussion

3.1. H_2 2.12 μm emission

Fig. 1 shows a map of the H_2 emission towards IRAS 16547−4247. There is a complex chain of emission with three major concentrations (labeled A to C). Several of the brightest emission knots within each concentration have been labeled and their coordinates and fluxes are given in Table 1. The projected distance between the two outermost knots (A4 and C2) is 110 arcsec (1.5 pc at the distance of 2.9 kpc, Bronfman private communication). Both of these knots are approximately symmetrically offset from the radio jet detected by Garay et al. (2003). No emission arising from the Brγ line was detected.

The H_2 emission has the morphological characteristics of HH objects arising from the interaction of a collimated flow with the ambient medium. Concentration A has several knots in the shape of bow-shocks, all pointing away from the direction of the radio jet. Their arrangement is consistent with an elongated outflow cavity. Another series of emission knots may exist further north but is difficult to distinguish against the artifacts from the bright star. The morphology of concentration B is more complex and consists of two main emission structures. Both structures appear to delineate flows originating from a direction that is skewed from the location of the radio jet: one in a northeast–southwest direction (B1, B2, and B6) and one in a north–south direction (B3, B4 and B5). This may be evidence of additional outflows from less-massive stars or an indication of precession of the flow originating from the detected radio jet. There are fewer bright emission knots in concentration C and the morphology is less well-defined. There are a couple of faint filaments in the shape of bow-shocks pointing away from the direction of the radio jet. These are most likely part of the counter-flow to concentration A.

Fig. 2 illustrates the comparison between the H_2 emission (without any continuum subtraction) and (a) the 1.2-mm dust continuum emission and (b) the 8.6-GHz continuum emission taken from Garay et al. (2003). The actual thermal radio jet corresponds to the brightest 8.6-GHz emission component. There is a fainter source offset to the southeast and whose spectral index is not known. It is not certain what role (if any) this source plays. The chain of H_2 emission is oriented in the same direction as the triple radio source and is contained within the molecular core traced by the 1.2-mm continuum emission. One of the H_2 emission knots (B1) is associated with the southern non-thermal radio component. The striking alignment of the collimated flow delineated by the H_2 emission and the central

location of the radio jet implies that these phenomena are coupled. It is reasonable to assume that the radio jet is the driving force of the collimated flow. No stellar counterpart to the radio jet was detected in the narrow-band near-infrared images (e.g. see Fig. 2b).

IRAS 16547−4247 is reminiscent of another young massive stellar object, HH80-81 ($\approx 1.7 \times 10^4$ $L_\odot$ at 1.7 kpc). HH80-81 contains a thermal radio jet centred on a collimated HH flow that extends over 5 pc (Martí et al. 1993). Evidence for non-thermal radio emission has also been reported towards one of the HH emission knots. Up until now this was the most luminous young stellar object known to have a collimated jet.

3.2. 11.9-μm emission

The 11.9-μm image obtained in this study reveals a single unresolved ($< 0.6\,''$) emission source with a flux of 0.28 Jy, albeit there may be less-luminous objects present that are below the sensitivity limit of the observations. Within the positional uncertainty of the mid-infrared data, this source is coincident with the radio jet. The flux is consistent with the spectral energy distribution for IRAS 16547−4247 shown in Garay et al. (2003).

According to the relationship between jet radio-luminosity and outflow momentum rate reported by Anglada et al. (1998), extrapolated to the high-mass regime, the IRAS 16547–4247 outflow should have a momentum rate of 0.2 $M_\odot$ yr^{-1} km s^{-1}. This mechanical force can only be supplied by a driving source with a luminosity of $\approx 10^5$ $L_\odot$ (Beuther et al. 2002). The measured luminosity for IRAS 16547–4247 is 6.2×10^4 $L_\odot$. Therefore we argue that the radio jet and the H_2 collimated flow are powered by the same single luminous object. Furthermore, it is reasonable to suppose that the detected 11.9-μm emission source is associated with this luminous object.

4. Conclusions

IRAS 16547−4247 is the most luminous embedded pre-main sequence source in the Galaxy known to harbor a thermal radio jet. We have detected a chain of H_2 2.12 μm emission knots towards IRAS 16547−4247 that delineate a collimated flow extending over 1.5 pc. The geometry of the flow implies that it is driven by the thermal jet. We have also identified an isolated unresolved mid-infrared object associated with the jet that is likely to be responsible for the excitation of IRAS 16547−4247. If the luminosity of IRAS 16547–4247 comes from a single object it would have the spectral type O8. The finding of a jet and collimated flow towards such a massive object supports the accretion scenario for the

formation of stars across the entire mass spectrum.

We thank Vanessa Doublier, Rachel Johnson, Nathan Smith and Michael Sterzik for their help with observations and data reduction. The ISAAC data were obtained through the ESO Director's Discretionary Time Program. This work has been partly funded by the Chilean Centro de Astrofísica FONDAP N^{o}15010003.

REFERENCES

Anglada, G., Villuendas, E., Estalella, R., Beltrán, M. T., Rodríguez, L. F., Torrelles, J. M., & Curiel, S. 1998, AJ, 116, 2953

Beuther, H., Schilke, P., Sridharan, T.K., Menten, K.M., Walmsley, C. M., & Wyrowski, F. 2002 A&A, 383, 892

Bonnell, I. A., Bate, M. R., & Zinnecker, H. 1998, MNRAS, 298, 93

Caswell, J. L. 1998, MNRAS, 297, 215

Cuby, J. G., Barucci, A., de Bergh, C., Emsellem, E., Moorwood, A. F., Petr, M., Pettini, M., & Tresse, L. 2000, SPIE, 4005, 212

Forster, J. R. & Caswell, J. L. 1989, A&A, 213, 339

Garay, G., Brooks, K. J., Mardones, D., Norris, R P. & G., B. M. 2002, ApJ, 579, 678

Garay, G., Brooks, K. J., Mardones, D., & Norris, R. P. 2003, ApJ, 587, 739

Martí, J., Rodríguez, L. F., & Reipurth, B. 1993, ApJ, 416, 208

McKee, C. F. & Tan, J. C. 2003, ApJ, 585, 850

Osorio, M., Lizano, S., & D'Alessio, P. 1999, ApJ, 525, 808

Reimann, H.-G., Linz, H., Wagner, R., Relke, H., Kaeufl, H. U., Dietzsch, E., Sperl, M., & Hron, J. 2000, SPIE, 4008, 1132

Reipurth, B. & Bally, J. 2001, ARevA&A, 2001, 39

Reipurth, B., Heathcote, S., Morse, J., Hartigan, P., & Bally, J. 2002, AJ, 123, 362

Rodríguez, L. F. 1997, in Herbig-Haro Flows and the Birth of Stars; IAU Symposium No. 182, ed. B. Reipurth & C. Bertout (Netherlands: Kluwer Academic Publishers), 83

Table 1. Flux parameters for the H_2 2.12 μm knots identified in Fig. 1.

	Peak Position		Peak Flux	Total Flux[a]
	RA(J2000)	Dec(J2000)	$\times 10^{-15}$ erg s^{-1}	$\times 10^{-14}$
	h m s	° ′ ″	cm^{-2} arcsec^{-2}	erg s^{-1} cm^{-2}
A1	16 58 17.2	−42 51 43	11	5.0
A2	16 58 16.5	−42 51 38	5.1	4.5
A3	16 58 16.9	−42 51 34	2.6	1.4
A4	16 58 16.5	−42 51 26	4.1	1.3
A5	16 58 16.5	−42 51 31	5.8	3.6
B1	16 58 17.4	−42 52 16	3.3	1.7
B2	16 58 16.6	−42 52 17	3.6	1.6
B3	16 58 16.4	−42 52 25	31	9.3
B4	16 58 17.0	−42 52 35	4.3	3.7
B5	16 58 16.9	−42 52 39	3.6	1.1
B6	16 58 15.9	−42 52 24	2.1	0.4
C1	16 58 18.2	−42 52 59	3.4	0.8
C2	16 58 18.1	−42 53 12	2.1	0.5

[a]Each integrated over $\approx 4'' \times 4''$ box.

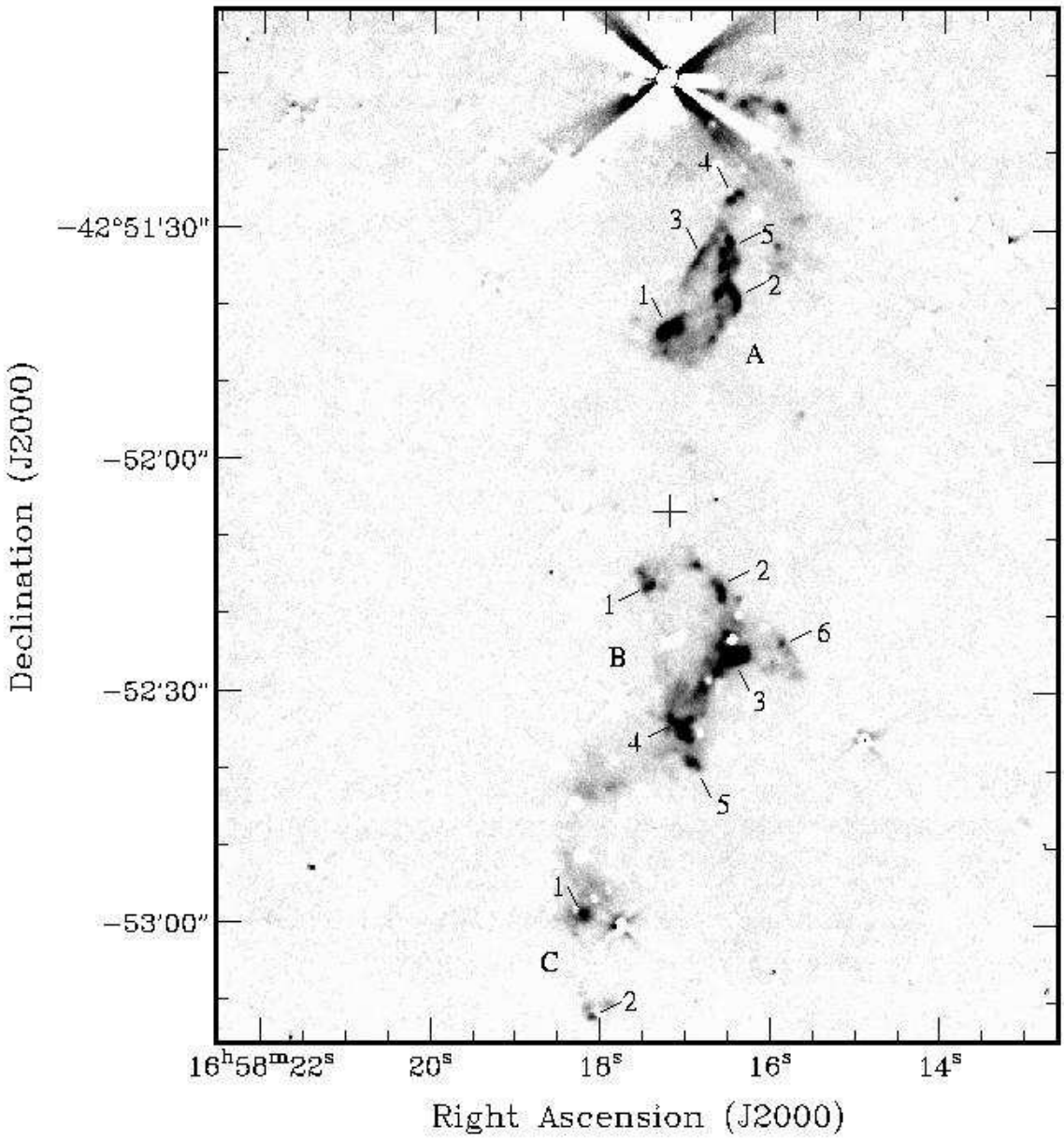

Fig. 1.— ISAAC H_2 2.12 μm emission image (continuum subtracted). A number of bright emission knots are labeled and their fluxes are listed in Table 1. The location of the thermal radio jet detected by Garay et al. (2003) is denoted by a cross (+). Artifacts at the top of the image are the result of an imperfect subtraction of the brightest star in the field.

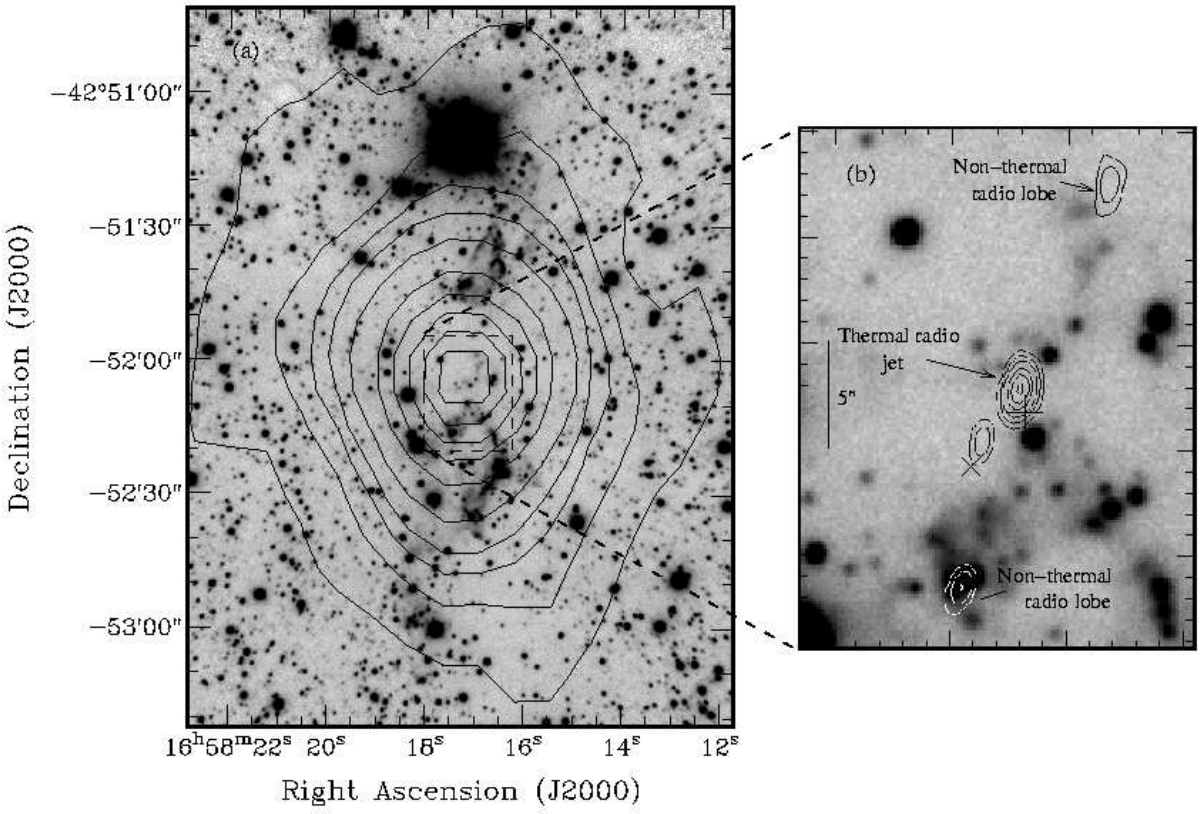

Fig. 2.— ISAAC H_2 2.12 μm emission image (no continuum subtraction) shown in grey scale. (a) Overlaid with 1.2-mm dust continuum emission from Garay et al. (2003). Contour levels are 0.25 (5σ), 0.5, 0.75, 1, 1.5, 2.5, 3.5, 4.5, 5.5, 6.5 Jy beam^{-1}. (b) Overlaid with 8.6-GHz continuum emission from Garay et al. 2003. Contour levels are 0.35 (5σ), 0.6, 1.1, 2.3, 3.5, 5 mJy beam^{-1}. Also shown are the OH maser position (+) from Caswell (1998) and the H_2O maser position ($\times$) from Forster & Caswell (1989). There is a positional uncertainty of 1″ in registering the H_2 2.12 μm and 8.6-GHz continuum data.